Islamic Azad University

Journal of

Optoelectronical Nanostructures

Winter 2024 / Vol. 9, No. 4

Absorption Enhancement of Thin Film Solar Cell Utilizing a Graphene-Based Metasurface

Amir Mehrpanah [1], Hasan Rasooli Saghai [*, 2], Babak Sakkaki [3], Ali Daghigh [1]

[1]Department of Electrical Engineering, Shabestar Branch, Islamic Azad university, Shabestar, Iran

[2]Department of Electrical Engineering, Tabriz Branch, Islamic Azad university, Tabriz, Iran

[3]Department of Electrical Engineering, Miandoab Branch, Islamic Azad University, Miandoab, Iran

Received: **13 Sep. 2024**
Revised: **17 Oct. 2024**
Accepted: **30 Oct. 2024**
Published: **15 Nov. 2024**

Keywords:
Graphene nanoribbon,
Plasmonic effect,
Refractory metal

Abstract:

Thanks to the unique features of graphene, graphene-based metasurfaces have gained great attention in electronic applications. This manuscript introduces a graphene-based metasurface aiming absorption enhancement in thin film solar cells. We manipulate our design to induce the plasmonic effect in our metasurface. We optimize our metasurface with 2D-GNRs on the top of a SiO2 layer with a thickness of 60 nm. A thin film solar cell (TFSC) is designed based on Si utilizing 2D-GNRs/SiO2 nanostructure and its characteristics are compured with and without 2D GNRs utilizing the FDTD method. The optical short circuit current density increases from 10.66 mA/cm^2 to 19.07 mA/cm^2 and solar generation rate increases from $6.57\times10^{27}(1/m^3)/s$ to $2.62\times10^{28}(1/m^3)/s$ with 2D GNRs on the top of SiO_2.The plasmonic resonance peaks are reported at the wavelength of 567 nm and 680 nm. To minimize the transmission from TFSC and based on the transmission profile and solar generation rate, we propose Al as a reasonable and suitable choice for the bottom electrode.

Citation Amir Mehrpanah , Hasan Rasooli Saghai , Babak Sakkaki , Ali Daghigh. Absorption Enhancement of Thin Film Solar Cell Utilizing a Graphene-Based Metasurface. **Journal of Optoelectronical Nanostructures.**
DOI: 10.30495/JOPN.2024.33743.1330

***Corresponding author:** Hasan Rasooli Saghai
Address: Department of Electrical Engineering, Tabriz Branch, Islamic Azad university, Tabriz, Iran. ***Tell:*** *00989143156503* ***Email:*** *h_rasooli@iaut.ac.ir*

1. INTRODUCTION

For decades, metamaterials have attracted great attention because of their unnatural properties such as negative permittivity and permeability, perfect absorption, subwavelength focusing, asymmetric transmission, cross-polarization conversion and hyperbolically engineered dispersion that are not normally found in nature [1-3]. From laboratory concepts to practical engineering applications, metamaterial are able to control independently the amplitude, phase, polarization state/direction, and other features of the irradiated electromagnetic wave. Related to this category, novel planar devices and systems are developed working in different frequency bands such as low frequency, high frequency, microwave, THz, and visible light [4].

However, because of the fabrication complexity of 3D metamaterials, the high insertion loss in the bulk metamaterials, and significant ohmic losses at optical frequencies, they are being replaced by 2D unit cells with dimension of subwavelength, namely metasurfaces [5, 6]. In comparison to 3D metamaterials, metasurfaces are ultrathin, have low loss, and enable easy integration [7]. In addition, due to the confinement of the local field, metasurfaces can generate considerable near-field effects [5]. Regardless of the application, the accessible spectral range is largely dictated by the material choice for the metasurface building blocks. Also their features can be controlled through designing suitable geometrical parameters [8].

Graphene, a 2D hexagonal lattice of carbon atoms and tunable nanomaterial, has been considered as a suitable alternative for metasurface integration [9, 10]. This is because of Fermi level of graphene's sheet that is adjustable using an external electric field or chemical doping to resulting in a broad range modulated conductivity [11]. Also, it is well established that graphene plasmon polaritons can provide strong optical confinement [12]. Besides its quantum confinement and tunable conductivity, the outstanding features of graphene nanostructures such as graphene nanoribbon are under influence of their high edge/bulk ratio [13]. So graphene-based metasurfaces attracted extensive consideration because of their significant optoelectronic features, broadband absorption, and electronic tenability [14].

Many researchers have worked on the design, numerical solution, and simulation of graphene-based metasurfaces. Lerer et al. modeled a periodic multilayer graphene-dielectric metasurface for terahertz and far infrared applications. In the abovementioned study, the surface conductivity of graphene was computed using the Kubo formalism [15]. Parmer et al. proposed an absorber based on graphene that absorbs broadly in the ultraviolet and visible range. This absorber consists of three layers including a gold resonator, a graphene monolayer as a spacer, and a SiO2. This metasurface was analyzed applying the finite element method and a 94% absorption at the wavelength of 0.4 to 0.7 μm was reported [16]. Raad et al. designed and simulated a hollow nano-pillar based on graphene with the shell-style shape on top of a TiN substrate. Graphene nano-pillar acted as impedance matching element while TiN, as a refractory metal, blocked the light transmission from the metasurface. Kubo formulas and the model of Drude Lorentz were exploited to approximately calculate the surface conductivity and dispersive permittivity of graphene layer, respectively. the absorption efficiency was obtained above 96% at the frequency range of 200-1000 terahertz [17]. Nagandla et al. modulated the electromagnetic waves by a metasurface based on graphene.This metasurface contained three layers including bottom reflector layer of gold, a middle spacer layer of Si, and graphene as a conductive top layer [18].

In this study, we present a metasurface for absorption enhancement in thin film solar cells. Solar cells are promising eco-friendly energy source to decrease fossil fuels consumption[19]. Thin film cells are suitable replacement for crystal-based cells as they have lower production cost [20]. Our structure contains three layers, including graphene nanoribbons, a dielectric layer, and a refractory metal. Graphene nanoribbons are utilized to produce the plasmonic effect. Plasmonic effect is the oscillation of free electrons of a metal nanostructure under illumination of an electromagnetic wave. The plasmonic resonance will induce if the frequencies of the incident light and free electrons oscillation are equal. [21,22]. A plasmonic surface can scatter light toward a subwavelength area in many directions when is irradiated in its surface plasmon resonance (SPR). SPR is an optical phenomenon related to the interaction of irradiated light with free a metal nanostructure [22,23]. SPR boosts the light absorption by scattering light through a mechanism, namely the far-field scattering [24].

2. Material and method

Figure 1 depicts the proposed metasurface structure. This metasurface consists of three layers, including strips of graphene nanoribbon (GNR), a dielectric layer, and a refractory metal. The width of GNR strips is considered 50 nm. The thickness of graphene layer has been considered 0.5 nm and 1 nm by pioneering researchers [25]. But through synthesizing technology, graphene layers are separated by the thickness of 0.34 nm in graphite [26]. So in this work, we model the graphene as a thin layer of 3D material with the thickness of 0.34 nm and also as a 2D material

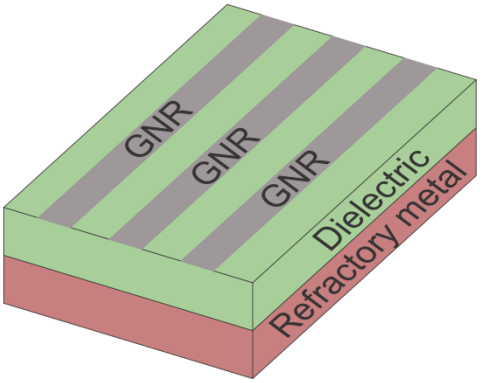

Fig. 1. The proposed metasurface structure.

A diagonal tensor models the anisotropic permittivity of graphene. Its surface-normal or out-of-plane dielectric constant is the same as the graphite dielectric constant and equals to 2.5. The in-plane dielectric constant of graphene is $\varepsilon_{xx}(\omega)=\varepsilon_{yy}(\omega)=2.5+i\sigma(\omega)/\varepsilon_0\omega T_G$. In this equation, ω, ε_0, T_G and $\sigma(\omega)$ are the angular frequency of incident light , the vacuum dielectric constant, the thickness and surface conductivity of graphene layer respectively [27,28]. The Kubo formalism is utilized to calculate the frequency dependent surface conductivity [28]. This formalism contains both inter and intra band terms of the graphene surface conductivity and is presented as following equation:

$$\sigma=\frac{i2e^2k_BT}{\pi\hbar^2\left(\omega+i\tau_G^{-1}\right)}+\frac{e^2}{4\hbar}\left[\frac{1}{2}+\frac{1}{\pi}\arctan\left(\frac{\hbar\omega-2E_f}{2k_BT}\right)-\frac{i}{2\pi}ln\frac{\left(\hbar\omega+2E_f\right)^2}{\left(\hbar\omega-2E_f\right)^2+4k_B^2T^2}\right] \quad (1)$$

where, e, k_B, $\hbar$, T, E_f, τ_G are the electron charge, the constant of Boltzmann, the reduced constant of Planck, the temperature, the graphene Fermi level, and the graphene carrier relaxation time respectively [28,29]. An external electric filed or a chemical doping are utilized to adjust the Fermi level [30]. We vary the graphene Fermi level from 0.3 eV to 1 eV. The Drude model is exploited to calculate τ_G through equation $\tau_G = \mu E_f / e\nu_f^2$. In this equation $\mu = 10000\, cm^2/V.s$ is the carrier mobility and $\nu_f = 10^8\, cm/s$ is Fermi velocity of carrier [28, 31,32].

As the plasmonic phenomenon occurs in metal/dielectric interface, the GNR strips are located on the top of a dielectric surface. The plasmon oscillation is not supported by zigzag GNRs. But metallic or insulating features can be obtained by armchair GNRs related to their width [33]. The permittivity of metallic GNRs with armchair-shape can be modeled via ab-initio and Kubo formalism. As mentioned above, we utilize the second approach in this study. To produce the SPR, different dielectrics related to metasurface design are replaced under GNR strips.

The refractory metal at the bottom of the structure is designed as the transmission blockage element. The absorbance characteristic of a structure is defined as $A(\omega) = 1 - R(\omega) - T(\omega)$ where, $R(\omega)$ and $T(\omega)$ are frequency dependent reflectance and transmittance, respectively [34].

With the optimal selection of the refractory metal, the transmission coefficient will have the minimum value. On the other hand, by optimal scattering from the surface toward the active layer, due to SPR effect, the reflectance coefficient will reach to its minimum value. Under this condition, the scattering parameters of S_{11} and S_{21} have to get minimize. As a result, the impedance of the surface $Z = (1+S_{11})/(1-S_{11})$ can be matched with free space impedance. Impedance matching is an important characteristic of a perfect metasurface absorber [17, 34].

For simulation process, in the first step, we design a two-layer surface, including GNR strips and a dielectric layer. This structure is irradiated by a TFSF source with a spectral range of 300 nm to 1100 nm as it is shown in figure 2. To obtain the best scattering cross section, we set two types of graphene including, 3D graphene with the thickness of 0.34 nm and 2D graphene, as the material of GNR. We swap the Fermi level of the GNRs from 0.3 eV to 1 eV. By variation of the Fermi level between 0.3~1 eV, graphene behavior changes from a dielectric with high loss to a metal without loss [35].

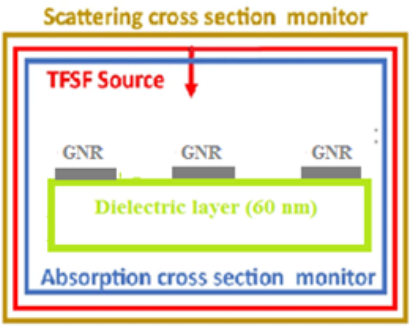

Fig. 2. The simulation demo of the GNR/dielectric structure.

Then we design a thin film solar cell (TFSC) utilizing the GNRs/dielectric surface with the best scattering cross section. Figure 3 shows this structure that is consisted of four layers, including GNR strips, a dielectric layer, a absorber layer of Si and the refractory metal as the bottom electrode. This structure is irradiated by a source of plane wave in the spectral range of 300 nm to 1100 nm in the direction of Z. Its characteristics are computed applying FDTD method. We put two field and power monitors at the above and below of the structure including reflection and transmission monitors. We the periodic boundary conditions are chosen along X and Y directions and PML boundary condition is chosen along Z direction. Finally, we use the solar generation rate solver for optical simulation. To obtain the minimum transmission, we change the material of the refractory metal

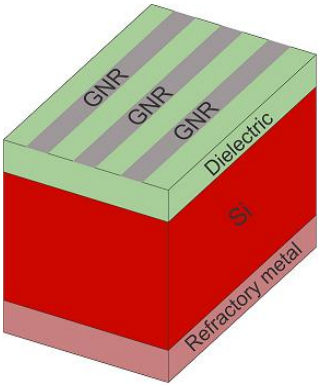

Fig. 3. The structure of the TFSC based on Si utilizing GNR metasurface.

.

Poynting theory is utilized to solve Maxwell equations to calculate the solar cell absorption through following equation:

$$P_{abs} = -0.5\omega|E|^2 \, img(\varepsilon) \quad (2)$$

where ω, |E| and *img* (ε) are angular frequency, the intensity of electric field, and the imaginary part of the permittivity, respectively [28,36,37]. We run our simulation under standard normalized spectrum AM 1.5. So the solar generation rate (G) and short circuit current density (J_{sc}) are obtained via following equations:

$$G(z) = \int_{300\,nm}^{1100\,nm} \frac{P_{abs}}{hc/\lambda} d\lambda \quad (3)$$

$$J_{sc} = e\int_{300\,nm}^{1100\,nm} \frac{\lambda}{hc} \frac{P_{abs}}{P_{in}} I_{AM.1.5}(\lambda) d\lambda \quad (4)$$

where, h is constant of Plank, c is the light speed, λ is wavelength, P_{in} is the irradiated light power, and $I_{AM1.5}$ is AM 1.5 solar spectrum [28,37-39]

3. Results and discussion

The structure of GNRs/dielectric is irradiated using TFSF source in the spectral range of 300 nm to 1100 nm and its scattering cross section is extracted using FDTD simulation. We try different materials as the dielectric layer, including SiO_2, Al_2O_3, and ZnSe. For GNR strips, we have two options, including 2D graphene and 3D graphene with E_f varying from 0.3 eV to 1 eV and T_G of 0.34 nm. To model 3D graphene ribbons, we utilize the isotropic permittivity which is extracted through $\varepsilon_{eq-G} = (\varepsilon_{zz}/3) + (2\varepsilon_{xx}/3)$, where ε_{eq-G} is the graphene equivalent permittivity, ε_{zz} is dielectric constant along Z direction and ε_{xx} is dielectric constant along X and Y directions. The simulation results reveal that the plasmonic effect induces at all GNRs/dielectric structures and cause a peak in the scattering cross section at different wavelengths. Because SiO_2 is one of the most common dielectrics in the design of solar cells, at this step, we chose to continue our study with this material.

The plasmonic effect, which is induced at the interface of GNRs and SiO_2 layer, is under the influence of not only the properties of GNRs but also the thickness of SiO_2. When the thickness of GNRs/SiO_2 is below 30 nm, the peak of scattering occurs beyond the wavelength of 300 nm. For GNRs/SiO_2 with the thickness of 40 nm, 60 nm, and 80 nm, the peaks of scattering are located at the wavelength of 426 nm, 538 nm, and 653 nm, respectively.

For GNRs/SiO_2 with a thickness of 100 nm, the peak of scattering is red-shifted forward 700 nm. According to the position of the scattering peaks, it seems that GNRs/SiO_2 with the thickness of 60 nm is a reasonable alternative for our study. Fig. 4 shows the scattering cross section of SiO_2, 3D-GNRs/SiO_2, and 2D-GNRs/SiO_2. The depicted results have come out by including 2D metallic GNRs and 3D GNRS with E_f=2.4 eV and T_G=0.34 nm.

According to Fig. 4, the scattering cross sections of GNRS/SiO_2 metasurface with 2D graphene ribbons have a higher peak. On the other hand, 3D graphene ribbons with lower E_f make a red shift at the position of the scattering peak. So at this step, we chose to continue our study with 2D graphene ribbons.

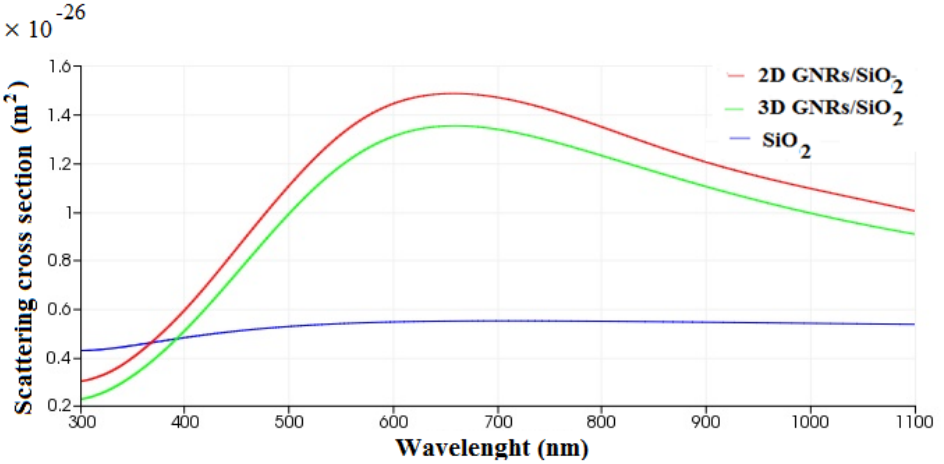

Fig. 4. The scattering cross section of SiO_2, 3D-GNRs/SiO_2 and 2D-GNRs/SiO_2.

Now, we simulate a standard TFSC and obtain its optical J_{sc} and G utilizing FDTD method. The abovementioned TFSC is consisted of three layers including SiO2 with the thickness of 60 nm, Si with the thickness of 300 nm, and Ag with the thicknesses of 100 nm. We compute the optical Jsc and G of this cell 10.66 mA/cm^2 and $6.57\times10^{27}(1/m^3)/s$, respectively. Then, to investigate the influence of our graphene-based metasurface on the performance of the TFSC, we add 2D GNRs at the top of the SiO_2 layer. Again, we calculate the characteristics of this solar cell. The optical J_{sc} increases to 19.07 mA/cm^2 and G rises to $2.62\times10^{28}(1/m^3)/s$.

Figure 5 shows the normalized absorption profile for these two solar cells. According to Fig. 5, the localized plasmonic resonance has three peaks at the wavelengths of 567 nm, 680 nm and, far infrared region. The third resonance is useless for solar cell applications. Figure 6 demonstrates the far field enhancement in a 50nm-unit cell at the wavelength of 680 nm without and with GNR strip at the top of SiO_2 layer

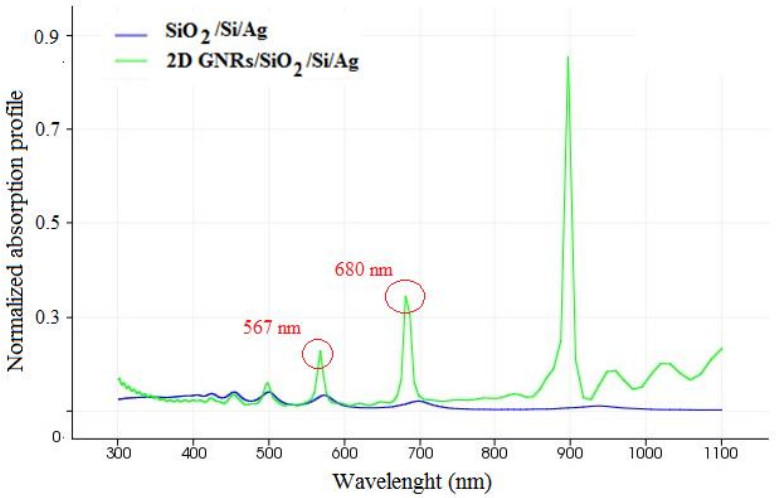

Fig. 5. The normalized absorption profile of a standard TFSC and TFSC with graphene-based metasurface.

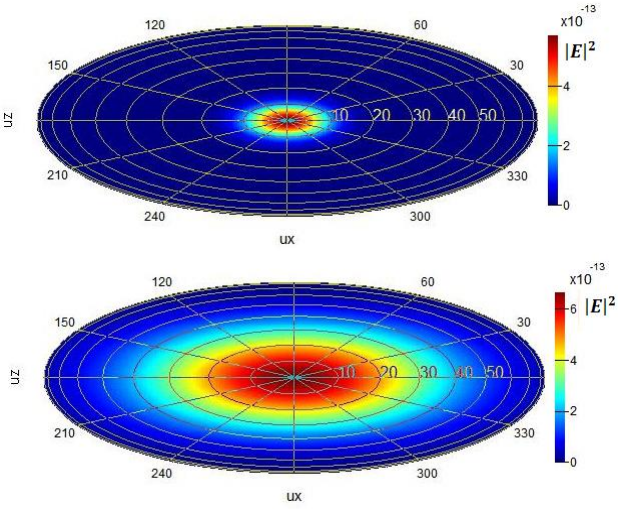

Fig. 6.The far field enhancement in a 50nm-unitcell at the wavelength of 680 nm (a): without GNR strip, (b): with GNR strip.

To find out the best alternative as the bottom layer of our structure, we extract the transmission cross section of TFSC with different refractory metals including Tungsten (W), Ag, Al, and TiN. Figure 7(a) presents the transmission cross section of TFSC with Tungsten and TiN bottom electrode and Figure 7(b) presents the transmission cross section of TFSC with Ag and Al bottom electrode. According to the Figure 7 the value of normalized transmission cross section in Figure 7(b) is much less that this value in Figure 7(a). According to Figure 7(b) the cell with Al bottom electrode has better transmission performance compared to the cell with Ag bottom electrode. So in this case, refractory metal of Al is chosen as the bottom layer of our metasurface and consequently as the bottom electrode of TFSC

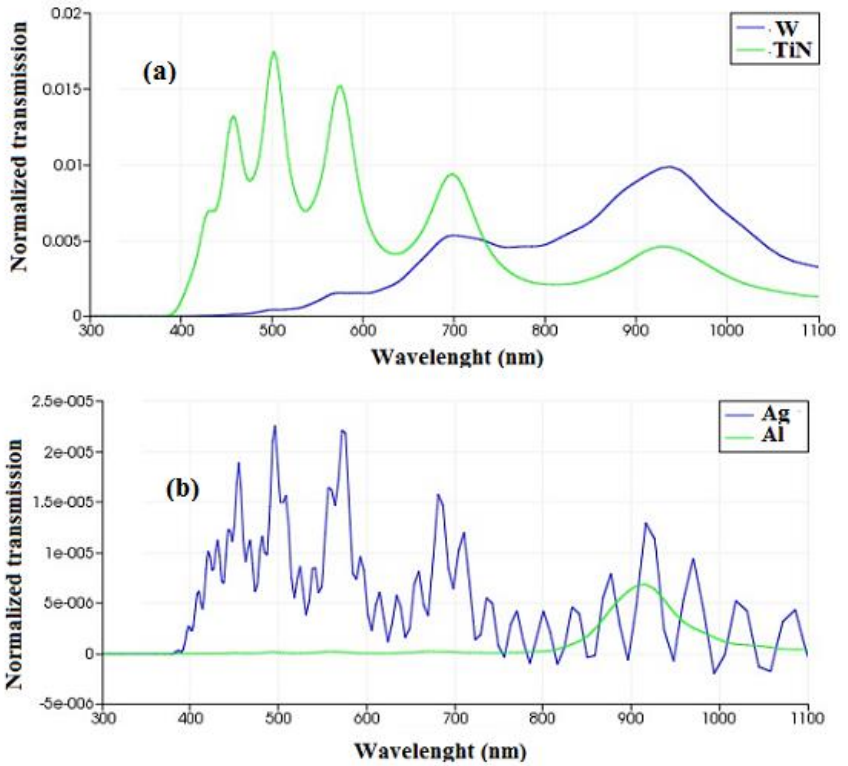

Fig. 7. The transmission cross section of TFSC with different refractory metals

4. Conclusion

In this research, we have introduced a graphene-based metasurface to absorption enhancement of TFSC. The metasurface consists of GNR strips with a width of 50 nm that are located on the top of a SiO_2 layer with a thickness of 60 nm. We have extracted the scattering cross section of GNRs/SiO_2 metasurface, considering GNR as 2D and 3D materials. To model the permittivity of 3D graphene ribbons, we have utilized the Kubo formalism considering E_f=0.3~1eV and T_G=0.34 nm. Under the irradiation of a TFSF source in the spectral region of 300 nm to 1100 nm, 2D-GNRs/SiO_2 structure has depicted a better scattering performance. To confirm the effect of the 2D-GNRs/SiO_2 metasurface on the absorbance of TFSCs, we have designed a TFSC based on our metasurface. This cell consists of 2D GNR strips, SiO_2 (60 nm), Si (300 nm), and refractory metal (100 nm). We have computed the characteristics of this cell through FDTD method with and without 2D GNR strips. The results of the simulation confirm that, by considering 2D GNR strips, the plasmonic resonance occurs at the wavelength of 567 nm and 680 nm. As a result, the optical J_{sc} increases from10.66 mA/cm^2 to 19.07 mA/cm^2 and G increases from $6.57\times10^{27}(1/m^3)/s$ to $2.62\times10^{28}(1/m^3)/s$.

Finally, we have extracted the transmission profile of the mentioned TFSC with different refractory metals. Although TiN has a better performance in reflecting light towards the active layer of the solar cell, the calculating of G reveal that Al is a better alternative for the bottom layer.

REFERENCES

[1] Ali, A., A. Mitra, and B. Aïssa. *Metamaterials and metasurfaces: A review from the perspectives of materials, mechanisms and advanced metadevices*. *Nanomaterials*. [Online]. *12*(6):1027(2022,Mar). available: https://doi.org/10.3390/nano12061027

[2] Lee, C.-W., H.J. Choi, and H. Jeong. *Tunable metasurfaces for visible and SWIR applications*. Nano Convergence. [Online]. 7(1):3 (2020,December). available: DOI:10.1186/s40580-019-0213-2.

[3] Ghajarpour-Nobandegani, S., M.J. Karimi, and H. Rahimi. *Tunable Terahertz Absorber Based on Hexagonal Graphene Disk Array*. Journal of Optoelectronical Nanostructures. [Online]. 8(2)(2023,May). available: https://doi.org/10.30495/jopn.2023.31722.1286

[4] Zahra, S., L. Ma, W. Wang, J. Li, D. Chen, Y. Liu, Y. Zhou, N. Li, Y. Huang, and G. Wen. *Electromagnetic metasurfaces and reconfigurable metasurfaces: a review*. Frontiers in Physics. [Online]. 8(8)(2021,January). available: https://doi.org/10.3389/fphy.2020.593411

[5] Zhao, X., Z. Sun, L. Zhang, Z. Wang, R. Xie, J. Zhao, R. You, and Z. You. *Review on metasurfaces: an alternative approach to advanced devices and instruments*. Advanced Devices & Instrumentation. [Online]. 13:1-19(2022). available:doi.org/10.34133/2022/9765089

[6] Joy, V., A. Dileep, P. Abhilash, R.U. Nair, and H. Singh. *Metasurfaces for stealth applications: A comprehensive review*. Journal of Electronic Materials. [Online]. 50(6) (2021,April). available: DOI:10.1007/s11664-021-08927-3.

[7] Bai, L., Y.K. Liu, L. Xu, Z. Zhang, Q. Wang, W.X. Jiang, C.-W. Qiu, and T.J. Cui. *A Smart Metasurface for Electromagnetic Manipulation Based on Speech Recognition*. Engineering. [Online]. 22: p. 185-190 (2023,March). available: https://doi.org/10.1016/j.eng.2022.06.026

[8] Servatkhah, M. and H. Alaei. *The Effect of Antenna Movement and Material Properties on Electromagnetically Induced Transparency in a Two-Dimensional Metamaterials*. Journal of Optoelectronical Nanostructures. [Online]. 1(2): p. 31-38. (2016,July). available: https://dorl.net/dor/20.1001.1.24237361.2016.1.2.3.2

[9] Liu, C., F. Yang, X. Fu, J. Wu, and L. Zhang. *Programmable Manipulations of Terahertz Beams by Graphene-Based Metasurface With Both Amplitude and Phase Modulations*. Frontiers in Materials. [Online].9: 932773(2022,june). available: https://doi.org/10.3389/fmats.2022.932773

[10] Akbari Eshkalak, M. and R. Faez. *A Computational Study on the Performance of Graphene Nanoribbon Field Effect Transistor*. Journal of Optoelectronical Nanostructures. [Online]. 2(3): p. 1-12 (2017,Sep). available: https://dorl.net/dor/20.1001.1.24237361.2017.2.3.1.9

[11] Zhang, Y., Y. Feng, and J. Zhao. *Graphene-enabled tunable phase gradient metasurface for broadband dispersion manipulation of terahertz wave*. Micromachines. [Online]. 14(11): p. 2006 (2023,January). available: https://doi.org/10.3390/mi14112006

[12] Li, Y., M.R. Krisshnamurthi, W. Luo, A.K. Swan, X. Ling, and R. Paiella.*Graphene metasurfaces for terahertz wavefront shaping and light emission*. Optical Materials Express. [Online]. 12(12): p. 4528-4546 (2022). available: http://dx.doi.org/10.2139/ssrn.4533276

[13] Sarkhoush, M., H. Rasooli Saghai, and H. Soofi. *Design and simulation of type-I graphene/Si quantum dot superlattice for intermediate-band solar cell applications*. Frontiers of Optoelectronics. [Online]. 15(1): p. 42. (2022,October). available: https://doi.org/10.1007/s12200-022-00043-2

[14] Yager, T., G. Chikvaidze, Q. Wang, and Y. Fu.*Graphene Hybrid Metasurfaces for Mid-Infrared Molecular Sensors*. Nanomaterials. [Online].13(14): p. 2113. (2023,july). available: doi.org/10.3390/nano13142113

[15] Lerer, A., G. Kouzaev, and G. Makeeva. *Electrodynamic and Probabilistic Calculation of Performances of THz devices Based on Periodic Mtilayer Graphene-Dielectric Structures*. presented at 2020 Moscow Workshop on Electronic and Networking Technologies (MWENT). IEEE. [Online]. (2020,March). available: doi.org/10.1109/MWENT47943.2020.9067449

[16] Parmar, J., S.K. Patel, and V. Katkar. *Graphene-based metasurface solar absorber design with absorption prediction using machine learning*. Scientific Reports. [Online].12(1): p. 2609(2022,Febraury). available: http://dx.doi.org/10.1038/s41598-022-06687-6

[17] Raad, S.H. and Z. Atlasbaf. *Solar cell design using graphene-based hollow nano-pillars*. Scientific Reports. [Online]. 11(1): p. 16169 (2021,August). available: https://www.nature.com/articles/s41598-021-95684-2

[18] Nagandla, P., P. Pokkunuri, and B. Madhav. *Graphene metasurface based broad band absorber for terahertz sensing applications. Measurement*: Sensors. [Online]. 30: p. 100927 (2023,December). available: http://dx.doi.org/10.1016/j.measen.2023.100927

[19] Sefidgar, Y., H. Rasooli Saghai, and H. Ghatei Khiabani Azar. *Enhancing Efficiency of Two-bond Solar Cells Based on GaAs/InGaP*. Journal of Optoelectronical Nanostructures. [Online]. 4(2): p. 83-

102(2019,jun). available:
https://dorl.net/dor/20.1001.1.24237361.2019.4.2.7.7

[20] Parcham, E. and S.A. Miandoab. *Introducing nanostructure patterns for performance enhancement in PbS colloidal quantum dot solar cells.* International Journal of Nano Dimension. [Online]. 11(1): p. 18-25.(2019,October). available:
dorl.net/dor/20.1001.1.20088868.2020.11.1.3.1

[21] Jangjoy, A., H. Bahador, and H. Heidarzadeh. *Design of an ultra-thin silicon solar cell using localized surface plasmonic effects of embedded paired nanoparticles*. Optics Communications. [Online]. 450: p. 216-221(2019,November). available:
https://doi.org/10.1016/j.optcom.2019.06.007

[22] Kanani, H., S. Golmohammadi, H.R. Saghai, and J. Pouladi. *Design of Graphene-Coated Silver Nanoparticle Based on Numerical Solution to Enhance the Absorption of the Thin-Film Solar Cell*. Plasmonics: [Online]. p. 1-9(2024,February). available:
http://dx.doi.org/10.1007/s11468-024-02231-6

[23] Heidary Orojloo, M., M. Jabbari, G. Solookinejad, and F. Sohrabi *Design and modeling of photonic crystal Absorber by using Gold and graphene films*. Journal of Optoelectronical Nanostructures. [Online]. 7(2): p. 1-10(2022,May). available:
https://doi.org/10.30495/jopn.2022.28915.1235

[24] Li, X., W. Yang, J. Deng, and Y. Lin. *Surface plasmon resonance effects of silver nanoparticles in graphene-based dye-sensitized solar cells.* Frontiers in Materials. [Online].10: p. 1137771(2023,May) available: doi:10.3389/fmats.2023.1137771

[25] Cao, S., T. Wang, Q. Sun, Y. Tang, B. Hu, U. Levy, and W. Yu.*Graphene–silver hybrid metamaterial for tunable and high absorption at mid-infrared waveband*. IEEE Photonics Technology Letters. [Online].30(5): p. 475-478(2018,March). available:
https://doi.org/10.1109/LPT.2018.2800729

[26] Chorsi, H.T. and S.D. Gedney.*Tunable plasmonic optoelectronic devices based on graphene metasurfaces*. IEEE Photonics Technology

Letters. [Online]. 29(2): p. 228-230(20167,January).available: http://dx.doi.org/10.1109/LPT.2016.263681

[27] Slizovskiy, S., A. Garcia-Ruiz, A.I. Berdyugin, N. Xin, T. Taniguchi, K. Watanabe, A.K. Geim, N.D. Drummond, and V.I. Fal'ko.*Out-of-plane dielectric susceptibility of graphene in twistronic and Bernal bilayers*. Nano Letters. [Online]. 21(15): p. 6678-6683(2021,August). availale: http://dx.doi.org/10.1021/acs.nanolett.1c02211

[28] Mehrpanah, A., H.R. Saghai, B. Sakkaki, and A. Daghigh. *Design of Graphene-Based Core/Shell Nanoparticles to Enhance the Absorption of Thin Film Solar Cells.* Plasmonics.[Online]. p. 1-7(2024,September). available: http://dx.doi.org/10.1007/s11468-024-02476-1

[29] Prokopeva, L.J., D. Wang, Z.A. Kudyshev, and A.V. Kildishev. *Computationally efficient surface conductivity graphene model for active metadevices*. IEEE Transactions on Antennas and Propagation. [Online].68(3): p. 1825-1835(2020, March). available: http://dx.doi.org/10.1109/TAP.2020.2967335

[30] Shi, Z., Y. Yang, L. Gan, and Z.-Y. Li. *Broadband tunability of surface plasmon resonance in graphene-coating silica nanoparticles*. Chinese Physics B. [Online].25(5): p. 057803(2016,April). available: http://dx.doi.org/10.1088/1674-1056/25/5/057803

[31] Liu, J.-X., Y.-J. Gao, W.-C. Tang, and H.-W. Yang. *A research of drude-two-critical points model of graphene near the optical frequency*. Superlattices and Microstructures. [Online]. 148: p. 106692(2020,December). available: http://dx.doi.org/10.1016/j.spmi.2020.106692

[32] Figueiredo, J.L., J.P. Bizarro, and H. Terças.*Weyl–Wigner description of massless Dirac plasmas: ab initio quantum plasmonics for monolayer graphene*. New Journal of Physics. [Online]. 24(2): p. 023026(2022, February).available: http://dx.doi.org/10.1088/1367-2630/ac5132

[33] Sindona, A., M. Pisarra, G. Falcone, C.V. Gomez, F. Mazzei, G. Cistaro, and S. Bellucci. *Plasmon properties of doped or gated graphene nanoribbon arrays with armchair shaped edges*. presented at IEEE MTT-S International Microwave Workshop Series on Advanced Materials and Processes for RF and THz Applications (IMWS-AMP).

IEEE. [Online].(2017, September).available: http://dx.doi.org/10.1109/IMWS-AMP.2017.8247337

[34] Hossain, M.J., M.R.I. Faruque, and M.T. Islam. *Correction: Perfect metamaterial absorber with high fractional bandwidth for solar energy harvesting*. PLoS One. [Online]. 14(1): p. e0211751(2018,November). available: http://dx.doi.org/10.1371/journal.pone.0211751

[35] Sikdar, D. and M. Premaratne. *Electrically tunable directional spp propagation in gold-nanoparticle-assisted graphene nanoribbons.* presented at 2014 IEEE Photonics Conference. IEEE. [Online].(2014,October). available: https://doi.org/10.1109/IPCon.2014.6995378

[36] Tharwat, M.M., A. Almalki, and A.M. Mahros. *Plasmon-enhanced sunlight harvesting in thin-film solar cell by randomly distributed nanoparticle array*. Materials. [Online].14(6): p. 1380(2021,March). available: http://dx.doi.org/10.3390/ma14061380

[37] Heidarzadeh, H., A. Jangjoy, and H. Bahador.*Use of coupled Al-Ag bimetallic cylindrical nanoparticles to improve the photocurrent of a thin-film silicon solar cell*. Plasmonics. [Online]. 17(3): p. 1323-1329(2022,March). available: http://dx.doi.org/10.1007/s11468-022-01630-x

[38] Selmy, A.E., M. Soliman, and N.K. Allam. *Refractory plasmonics boost the performance of thin-film solar cells*. Emergent Materials. [Online]. 1(10): p. 185-191(2018,November). available: http://dx.doi.org/10.1007/s42247-018-0017-x

[39] Katyani, R. and S. Andalibi Miandoab.*Enhance efficiency in flat and nano roughness surface perovskite solar cells with the use of index near zero materials filter*. Optical and Quantum Electronics. [Online]. 53(9): p. 520(2021,August). available: https://link.springer.com/article/10.1007%2Fs11082-021-03161-x